“From Static to Dynamic”

Institute of Shock Physics, Imperial College
London, 2010

SHOCK-WAVE BEHAVIOR OF METALS IN & OUT OF STRUCTURE-UNSTABLE STATES

Yu.I. Meshcheryakov, A.K. Divakov, N.I. Zhigacheva, I.P. Makarevich, *B.K. Barakhtin

Institute for Problems of Mechanical Engineering Russian Academy of Sciences,
*Central Research Institute of Constructional Materials “Prometey”,
Saint-Petersburg, Russia


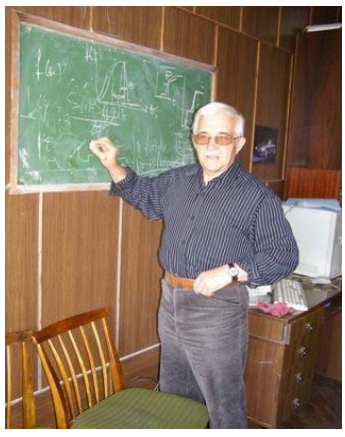


TEAM

MESO-MACRO MOMENTUM EXCHANGE

In the case of dynamic deformation, interaction between macroscale and mesoscale is realized through the following characteristics.

1).Particle velocity dispersion, D^2, the second statistical moment of the particle velocity distribution at the mesoscale

2). Defect of particle velocity, Δu, which determines a change of mean particle velocity at the macroscale as a result of transferring the energy and momentum from macroscale to mesoscale.

Both dynamic variables are on-line measurable, the first of them is of statistical nature whereas the second is deterministic. Universal soft coupling between macroscale and mesoscale is provided in the form *(Meshcheryakov, 2008)*

$$\Delta u = \frac{1}{2}\frac{d\left(D^2\right)}{du}, \qquad (1)$$

which is confirmed for variety of materials within wide range of strain rates.

Qualitative picture of meso-macro momentum exchange within steady plastic front is shown in ***Fig.1.*** During the first half of shock front the velocity defect decreases the mean velocity at the velocity profile whereas during the second half it increases the mean velocity so the velocity profile becomes steeper.

Physically, particle velocity dispersion, D^2, characterizes the energy of chaotic pulsations at mesoscale while the particle velocity defect, Δu is a measure of macroscopic momentum expanded on swinging the velocity pulsations. Eq. (1) can be written in the form:

$$\Delta u = D\frac{dD/dt}{du/dt} \qquad (2)$$

In the case

$$\frac{dD}{dt} = \frac{du}{dt}, \qquad (3)$$

i.e. when rate of change of velocity variation equals the rate of change of mean particle velocity, particle velocity defect equals to the particle velocity variation:

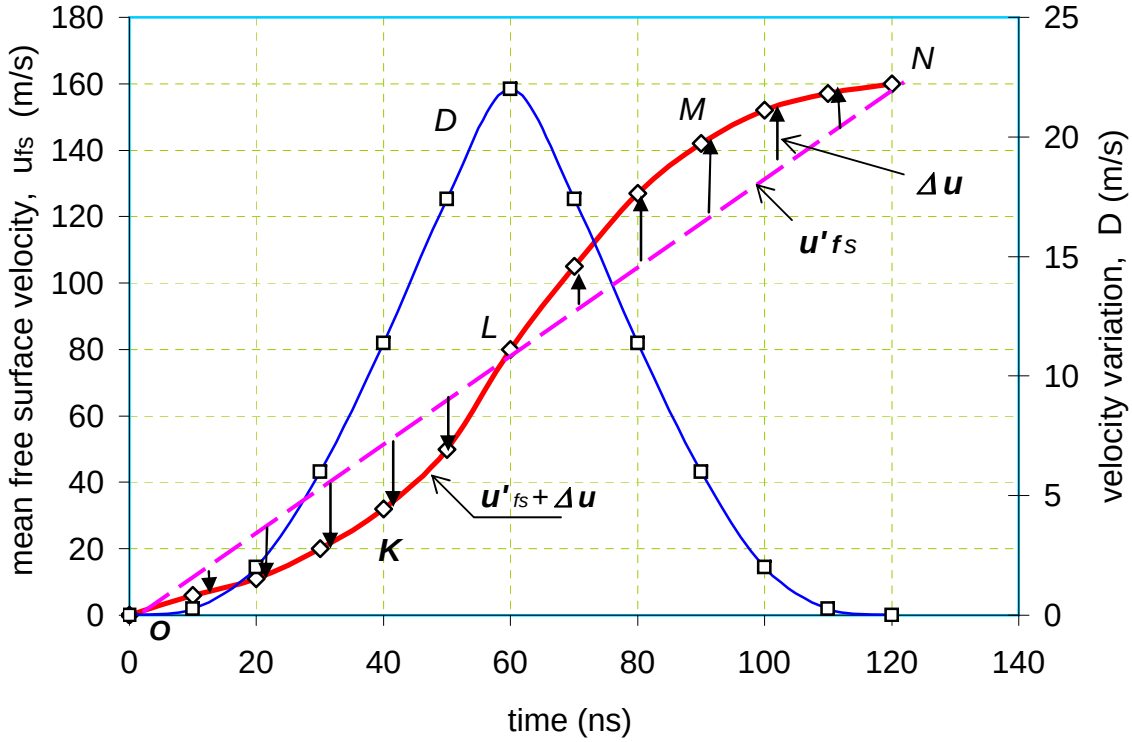
mean free surface velocity, ufs (m/s)
velocity variation, D (m/s)
time (ns)
0
20
40
60
80
100
120
140
160
180
5
10
15
25
D
M
N
L
K
O
Δu
u'fs
u'fs + Δu

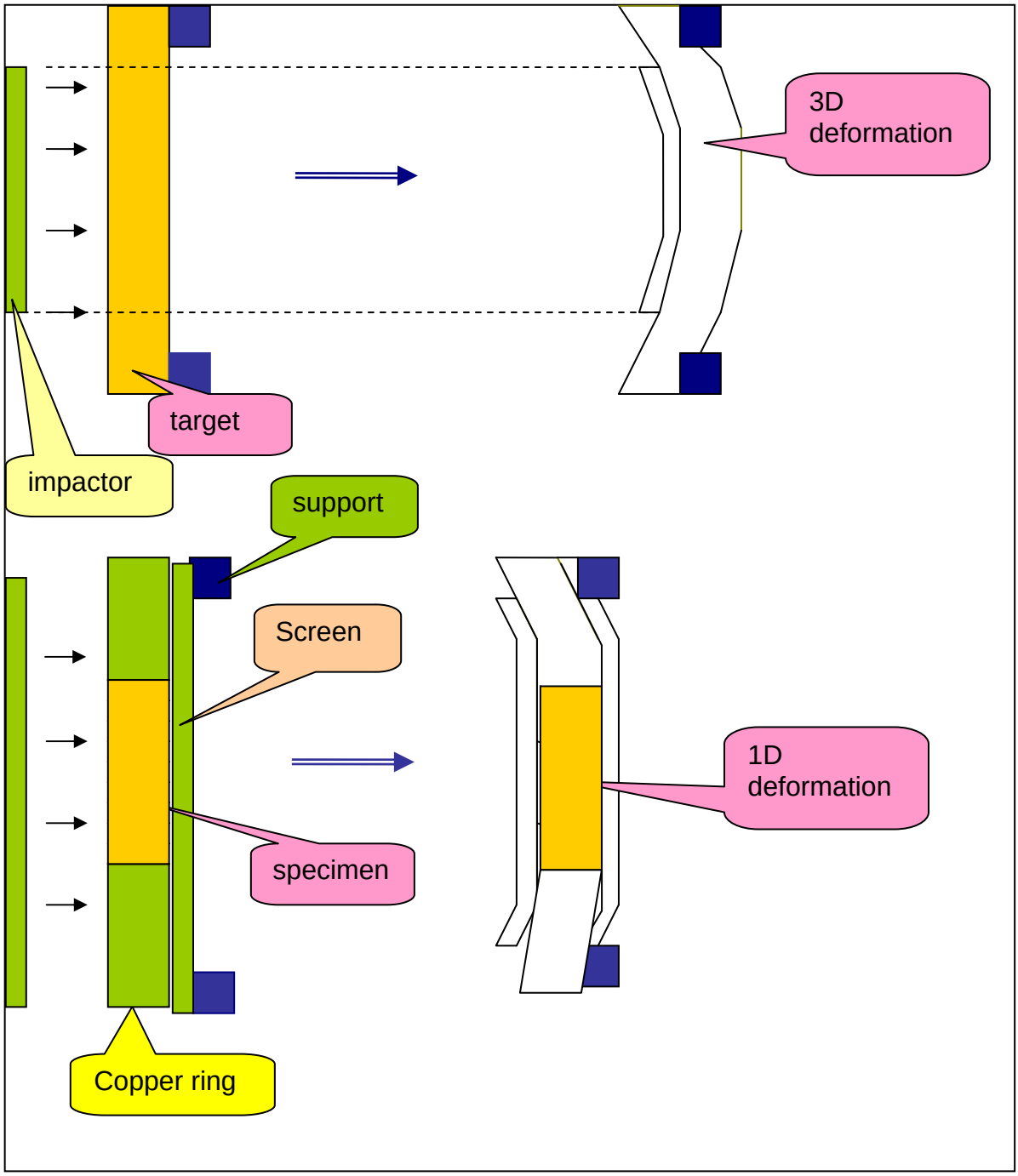
3D
deformation
target
impactor
support
Screen
specimen
1D
deformation
Copper ring

$$\Delta u = D \,. \tag{4}$$

After dividing the left and right hand sides by shock-wave speed $C_{0,}$

$$\frac{\Delta u}{C_0} = -\frac{D}{C_0}\frac{\dot{D}/C_0}{\dot{u}/C_0},$$

Eq. (3) can be written in terms of the strain and strain rates:

$$\Delta\varepsilon_{mc} = \varepsilon_D \frac{\dot{\varepsilon}_D}{\dot{\varepsilon}_{mc}} \,. \tag{5}$$

Here $\Delta\varepsilon_{mc}$ is a change of deformation at the macroscale due to energy exchange between macro- and mesoscales. This is addition to macro- deformation in expense of macro-meso energy exchange. ε_D and $\dot{\varepsilon}_D$ are the local deformation and rate of local deformation at the mesoscale resulted from particle velocity pulsations, ε_{mc} and $\dot{\varepsilon}_{mc}$ are the macroscopic deformation and rate of macroscopic deformation, respectively. Under condition

$$\dot{\varepsilon}_{mc} = \dot{\varepsilon}_D \,, \tag{6}$$

i.e. when strain rate at the macroscale equals the strain rate at the mesoscale, change of deformation at the macroscale equals deformation at the mesoscale:

$$\Delta\varepsilon_{mc} = \varepsilon_D \tag{7}$$

In shock experiments, directly measured values are the free surface velocity, u_{fs}, velocity defect, Δu, and particle velocity variation (square root of the particle velocity dispersion), $D,$ so the equations (3)-(4) can be directly verified. However, physical

meaning may be understood much better from equation (7) which is a condition for aligning the macroscopic and local strain rates.

This situation closely reminds the so-called ***"Kolmogorov's universal statistical equilibrium regime"*** of energy exchange in turbulence *(Hintze, 1962)*. This regime supposes that interaction between turbulent pulsations is absent and is determined by unit value of Reynolds number

$$\mathrm{Re} = \frac{\Delta u L}{\nu} = 1 . \qquad (8)$$

There are two aspects of transition of dynamically deformed solid into structure-unstable state.

1). Transition of solid into structure-unstable state is of statistical nature. This is a special kind of synergetic process which is known as a noise-induced phase transition.

2). Inertia of particles at the mesoscale must be higher than mean inertia of ensemble.

Both features follow from the criterion for transition into structure-unstable state *(Meshcheryakov et.al, 2008)*

$$\left(\frac{D}{u} \frac{\dot{D}}{\dot{u}} \right) \geq 1 . \qquad (9)$$

At the free surface velocity profile, transition into structure-unstable state looks as a break or cusp at the top of plastic front (see ***Fig.3***).

Shock tests of a variety of materials reveal two regimes of energy exchange between meso- and macro- scales - *evolutional and "catastrophic"* regimes. The latter regime supposes that mean particle velocity at the plastic front of compressive pulse at some strain rate stops to grow resulting in deficit (defect) of particle velocity. Physically, it means that energy obtained from external loading begins to expand on swinging the large-scale velocity pulsations. The criterion (9) declares that *transition from evolutional regime to catastrophic regime happens when rate of change of velocity variation becomes higher than rate of change of mean particle velocity.*

From the position of non-equilibrium statistical mechanics, asymmetry of the velocity distribution function means that kinematics of assemble of particles at the mesoscale is rotational. This directly follows from definition of kinetic stress tensor

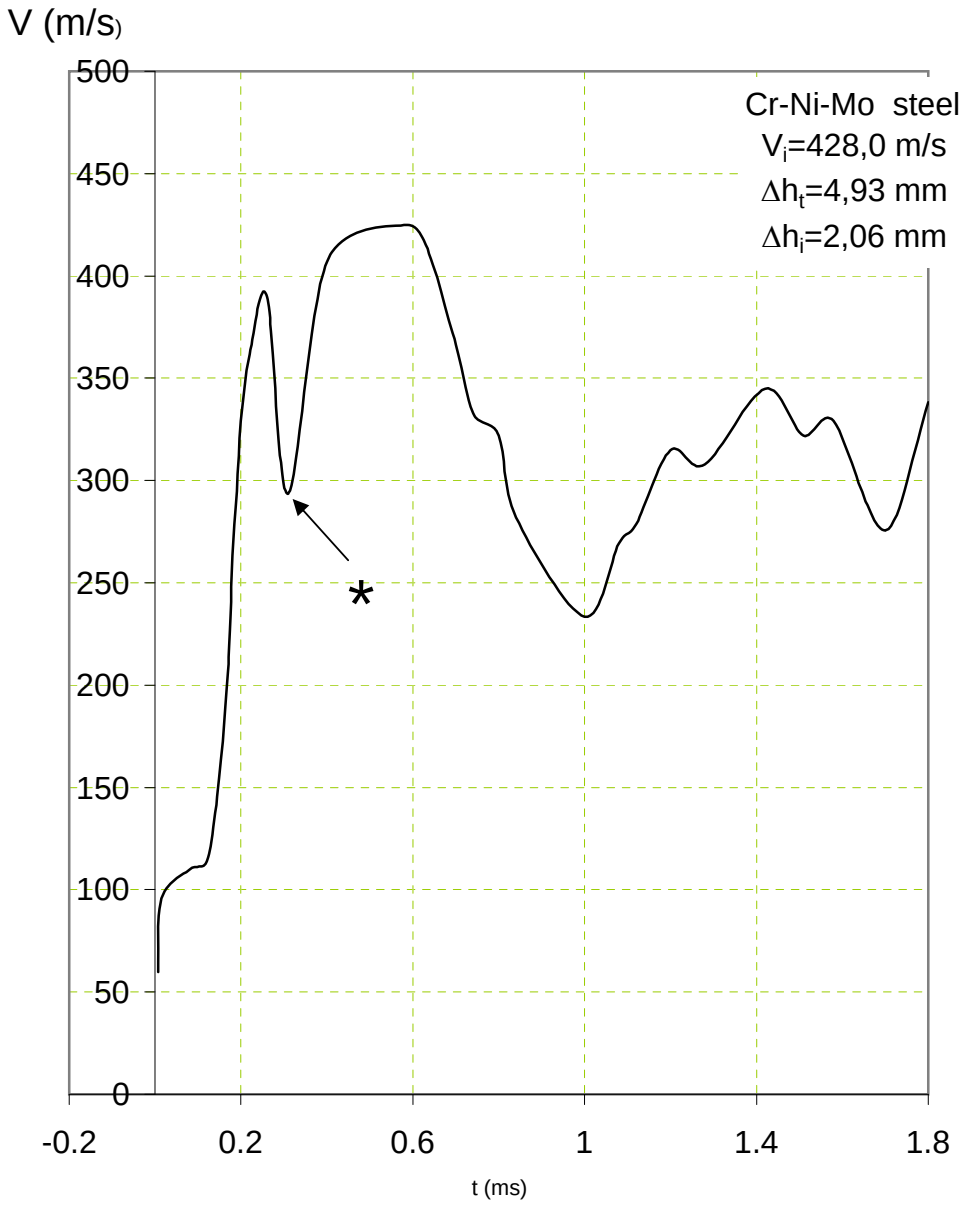

Figure 3. Free surface velocity profile for 30CrNi4Vo armor steel

which is introduced in kinetic theory as the second statistical moment of particle velocity distribution function:

$$P_{ik} = m\langle c_i c_k \rangle = v\int_{-\infty}^{\infty} c_i c_k f(v)dv \,, \tag{10}$$

where c_i and c_k are the components of relative particle velocities in directions x_i and x_k, respectively. For symmetrical velocity distribution function, such as Maxwell's distribution, rotational motion of medium at the mesoscale is not initiated, so $P_{ik} = 0$. Swinging of pulsation requires some time which is determined by non-local character deformation processes at the mesoscale. In this situation, by analogy with the mechanics of fracture *(Morozov et al., 1991)*, averaging of meso-macro energy exchange process may be accomplished in the form:

$$\frac{1}{\tau}\int_{t-\tau}^{t}\left(\frac{1}{2}\frac{\partial D^2}{\partial u}\right)ds \le \Delta U \,, \tag{11}$$

where τ is a time of averaging, which can be considered as "incubation time" of meso-macro energy exchange. In the case of equilibrium regime of meso-macro energy exchange, criterion (11) becomes:

$$\int_{t-\tau}^{t} D(s)ds \le \Delta U_{cr}\tau \,, \tag{12}$$

where ΔU_{cr} is a critical value of the velocity defect. Eq. (12) can be considered as a definition of a ***representative volume in the multiscale dynamic plasticity.*** Eq. (12) can be written in the form

$$\rho C_0 \int_{t-\tau}^{t} D(s)ds \le \Delta\sigma\tau \,, \tag{13}$$

where

$$\Delta\sigma\tau = \rho C_0 \Delta U_{cr}\tau \tag{14}$$

is ***elementary momentum*** transferred to mesoscale.

EXPERIMENTS

In experiments under uniaxial strain conditions there is a possibility for measuring an energy transferred from macroscale to mesoscale. Modern techniques for diagnostics of high-strain rate processes allow to register on-line at least three dynamic characteristics - mean particle velocity ***u(t),*** particle velocity dispersion $\boldsymbol{D^2(t)}$**,** as a sequence of velocity heterogeneity of dynamic deformation, and velocity defect $\Delta\boldsymbol{u(t)}$**.**

Two sets of M3 copper targets have been tested within impact velocities range 200 - 700 m/s. The fist set is all-in-one plane targets of 52 mm in diameter and 5 mm thick. When shocked, the targets suffered a small bending, so deformation was three-dimensional. Targets of second set were composed from 25 mm plugs mounted into 52 copper hoop. Macroscopic deformation of plug is one-dimensional and specimen was protected from repeating waves (Fig.2).

Fig. 4 presents dependencies of velocity variation D, velocity defect ΔU, and pull-back velocity W on the impact velocity U_{imp}.for M3 copper. Maximum pull-back velocity just corresponds to intersection of velocity variation and velocity defect curves. It means that maximum spall-strength is realized when momentum transferred from external load in the form of velocity defect equals the mean magnitude of velocity pulsations. Physically, equality of local strain rate at the mesoscale and macroscopic strain rate means that internal stresses have time to relax. Thus, the equilibrium regime of macro-meso energy exchange (3) corresponds to maximum dynamic strength.

Analogous results have been obtained for high-strength ductile steels. Dependencies of velocity variation, velocity defect and pull-back velocity on impact velocity for 45CrNiMoVNb steel are provided in ***Fig.5***. Equilibrium condition (3) allows to predict a regime of loading where plastic and strength properties of material are optimal. This was done for 40CrNiSiMoVNb steel. Result of tests in form of dependencies of pull-back velocity, velocity variation and velocity defect on the impact velocity are shown in ***Fig.6.*** At the beginning, the tests were carried out within impact velocity range of 200÷400 m/s where condition (3) isn't fulfilled. Extrapolation of velocity variation and velocity defect curves for higher impact velocity shows that their intersection occurs at the impact velocity of ~730 m/s, where maximum spall-strength

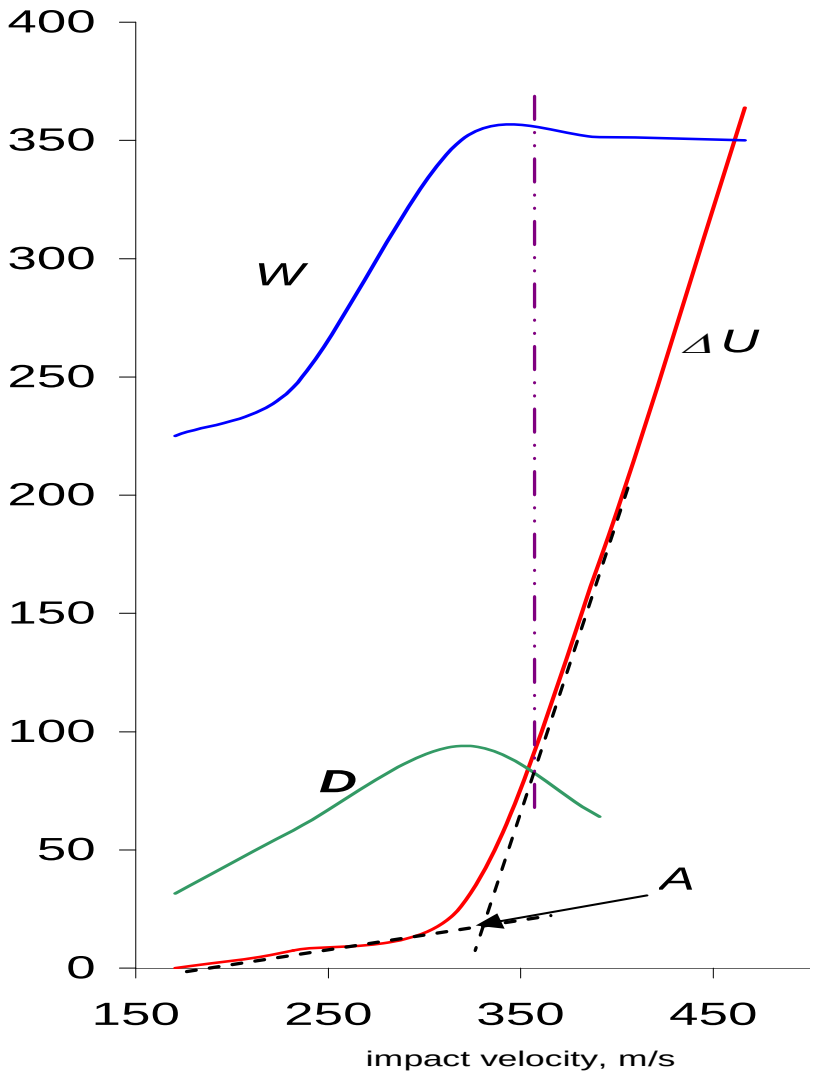

Figure 4. Velocity variation, D, velocity defect, ΔU, and pull-back velocity, W, versus impact velocity for M3 copper.

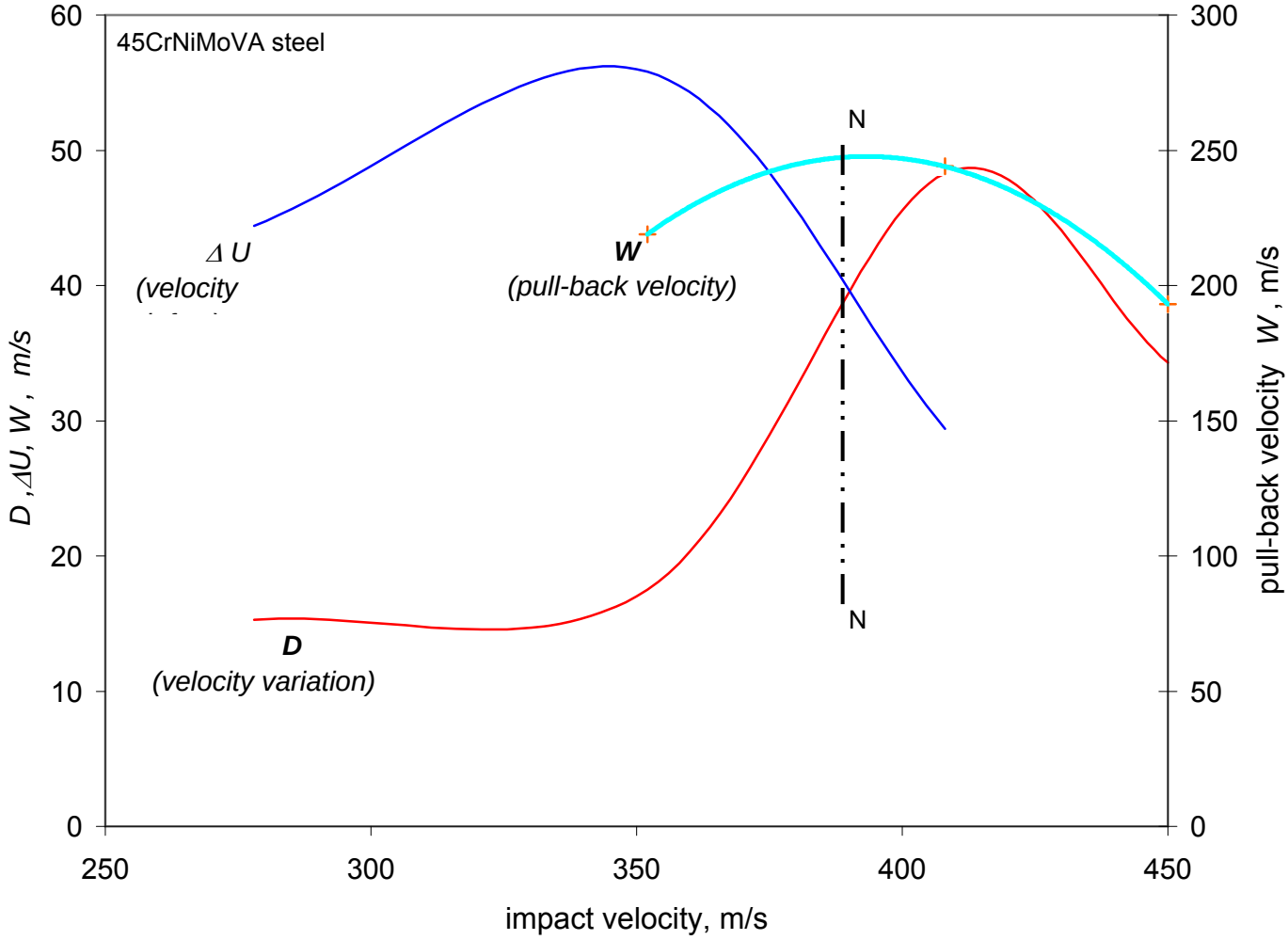

Figure 5. Velocity variation, D, velocity defect, ΔU, and pull-back velocity, W, versus impact velocity for 45KNMFA steel.

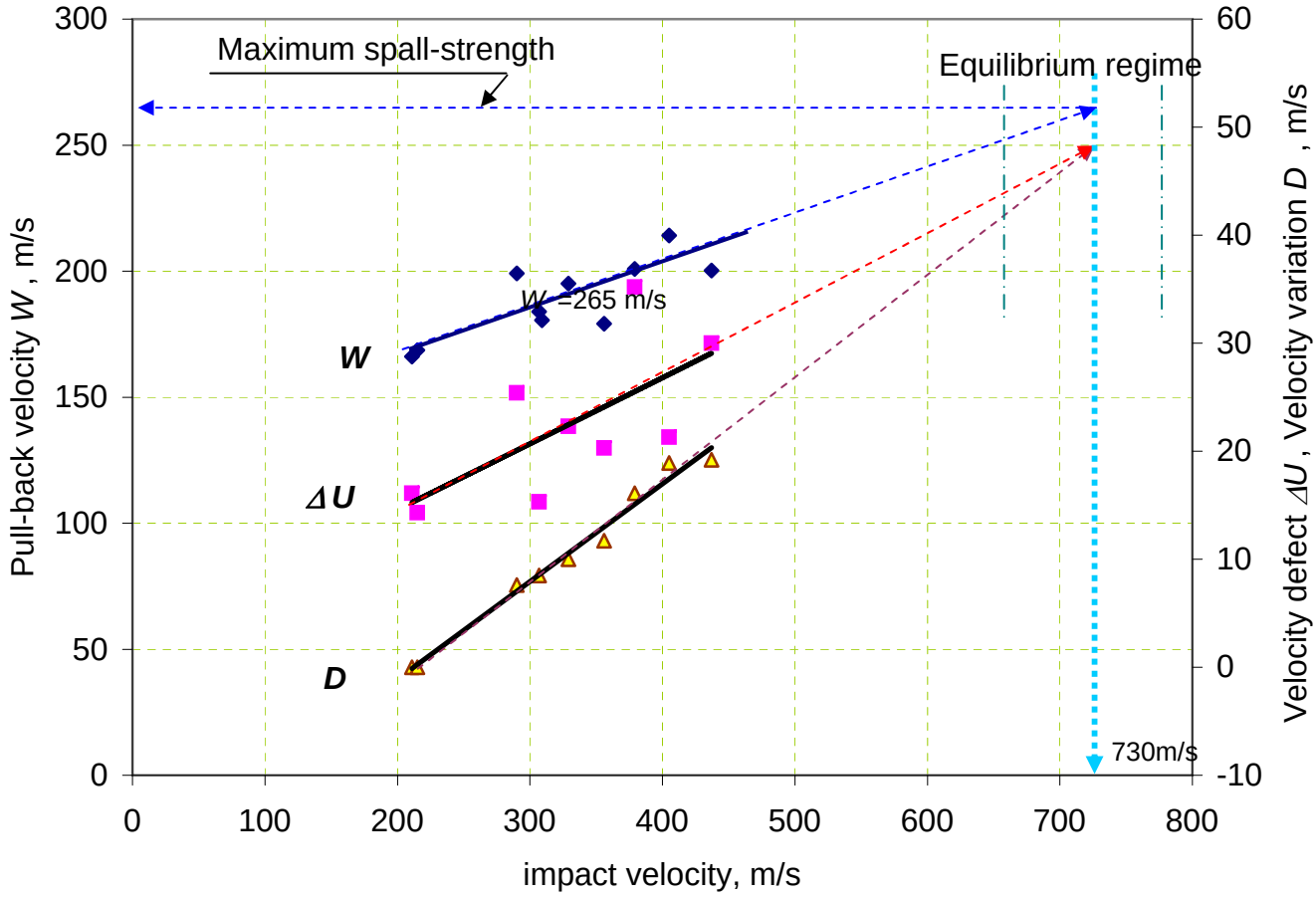

Figure 6. Velocity variation D, velocity defect ΔU and pull-back velocity W versus impact velocity for 40KHNSMA steel.

may be expected. To check this hypothesis, an additional test was performed at impact velocity of 730 m/s to determine a pull-back velocity. It turned out to be 265 m/s, i.e. by ~ 40 % higher than that for impact velocities of 250÷400 m/s. So, maximum dynamic strength for this steel is also realized under condition of equilibrium regime of meso-macro energy exchange when local strain rate equals macroscopic strain rate.

In case of M3 copper, dependence of spall-strength on the impact velocity has two regions. Below the impact velocity of ~170 m/s, pull-back velocity approximately equals 70 m/s. After impact velocity of 350 m/s it increases up to ~100 m/s. That valuable increase happens after transition into structure-unstable state which occurs at the impact velocity of 310 m/s.

Part of copper specimens was subjected to secondary loading. The targets preliminary loaded in scheme Fig.2*a*, were mounted in copper ring in scheme 2*b*. Secondary loading reveals a valuable increase of Hugoniot elastic limit and viscosity. For comparison, in ***Fig. 7*** two free surface velocity profiles are presented, both profiles are registered at close impact velocity of ~170 m/s. Curve *1* presents a time-resolved profile for initial material whereas the curve *2* is a profile for the material which suffered a shock loading at the impact velocity of 398 m/s after what it has been mounted into copper ring and again tested at the impact velocity of 170.6 m/s. Curve *2* demonstrates a seven-times increase of Hugoniot elastic limit and three-times increase of viscosity as compared to initial material. This increase is stipulated by change of defect structure caused by primary loading. At the same time, the value of spall-strength remains practically unchangeable (W_{sp} = 73.5 m/s), which can be explained that secondary loading was carried out below the threshold for structure-unstable state. Thus, in spite of valuable increase of dynamic yielding and viscosity caused by primary loading, spall-strength increases only in the case when material transits into equilibrium regime of structure-unstable state.

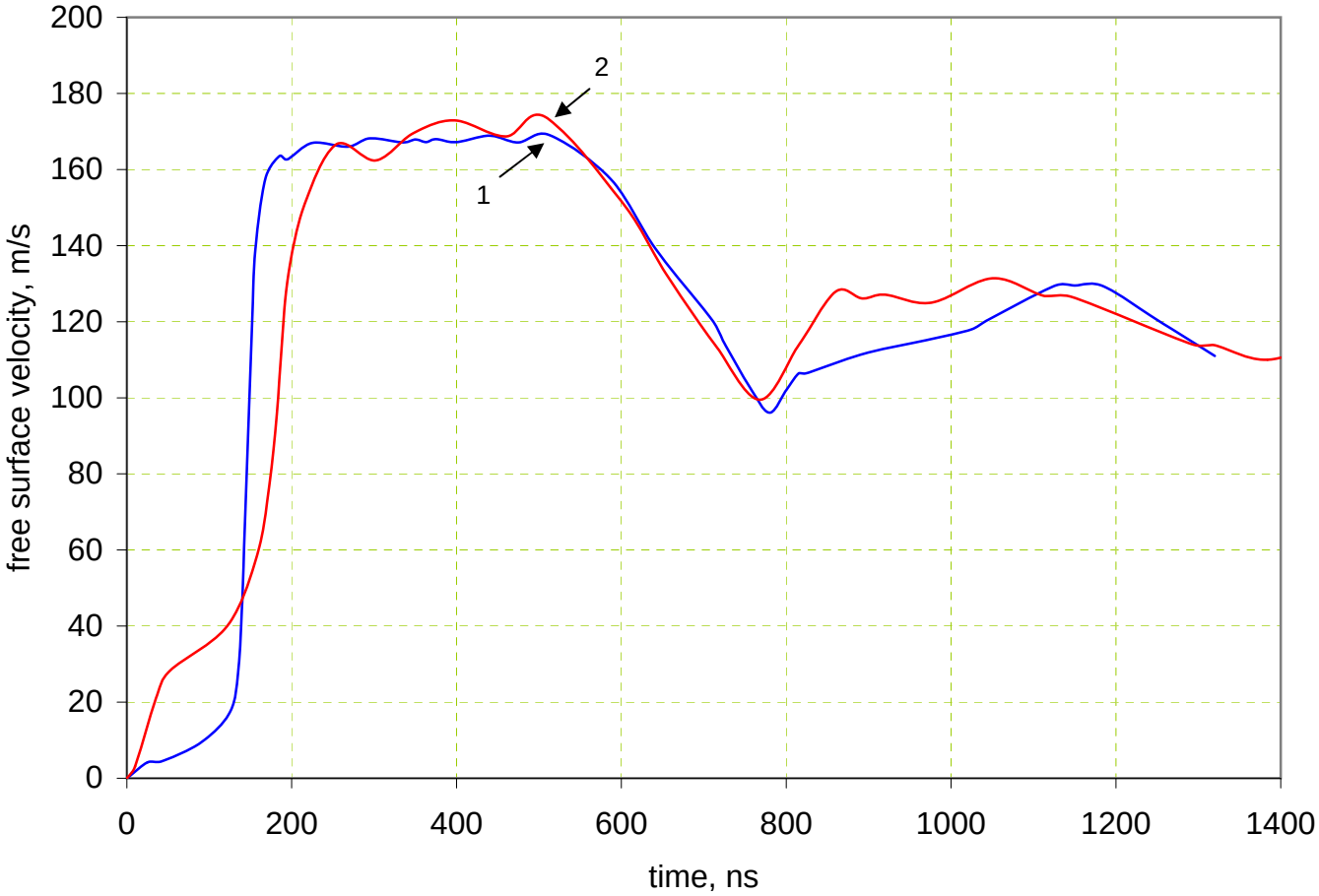

Figure 7. Free surface velocity profiles for M3 copper target: 1 loaded at the impact velocity of 170.4 m/s in initial state of material; 2 - after preliminary shock loading at the impact velocity of 398 m/s and repeated loading at the impact velocity of 170.6 m/s.

MESO-MACRO MOMENTUM EXCHANGE AND DYNAMIC PLASTICITY AND STRENGTH

In this Section, coupling between character of macro-micro energy exchange and dynamic plasticity and strength of solid is considered by comparing a dynamic response on impact for two metals. The first metal is Cr-Ni-Mo armor steel of 390HV hardness and the second metal is nitrogen austenitic 04Cr20Ni6Mn11Mo2NVNb of 254HV hardness (after hot deformation, tempering at 1100^0 C and cooling in water). Set of free surface velocity profiles for several impact velocities are provided in ***Fig.8(a,b).*** From comparison of profiles the following conclusions can be drown.

1). With increasing a strain rate, velocity profiles for Cr-Ni-Mo steel become steeper, whereas profiles for nitrogen steel don't change their inclination.

2). In Cr-Ni-Mo steel there is an evident particle velocity dispersion at the mesoscale, whereas in nitrogen steel the particle velocity dispersion is absent at all.

Swinging of large-scale velocity pulsations (quantitative characteristic of which is a velocity dispersion) evidences that transferring of momentum and energy from external load (macroscale) on to microscale flows through an intermediate (mesoscopic) scale. In opposite case, when particle velocity dispersion is absent, a direct transferring of momentum and energy from macroscale to microscale (atom-dislocation and microtwin scales) takes place.

In ***Fig. 9***, the dependencies of velocity defect for both kinds of steels are presented. For Cr-Ni-Mo steel the velocity defect is practically invariable, whereas for nitrogen steel, beginning from 310 m/s, it increases. In case of armor steel, threshold stress at what material transits into structure-unstable state increases with the increase of strain rate whereas for the nitrogen steel it remains invariable. By analogy with the behavior of liquid in turbulent regime of flow *(Hintze, 1962)*, the large-scale velocity pulsations in shock deformed solid play a role of intermediate mechanism which transfers momentum and energy from macroscale to level of elementary carriers of deformation - atom-dislocation scale. In the case of Cr-Ni-Mo steel, because of too large incubation time, the large-scale velocity pulsations delay irreversible stage of energy transferring,

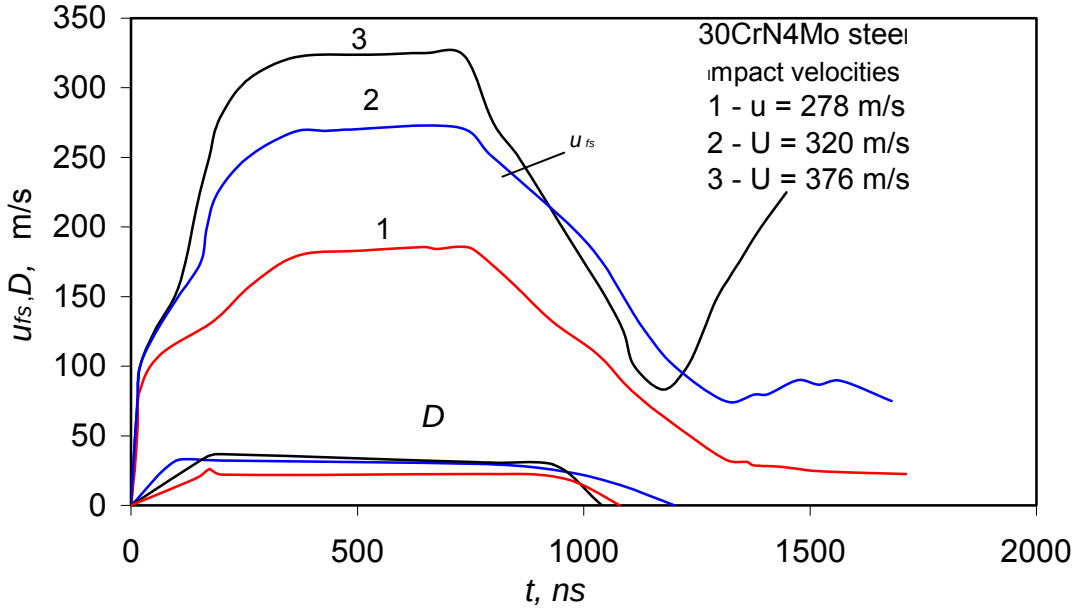

a)

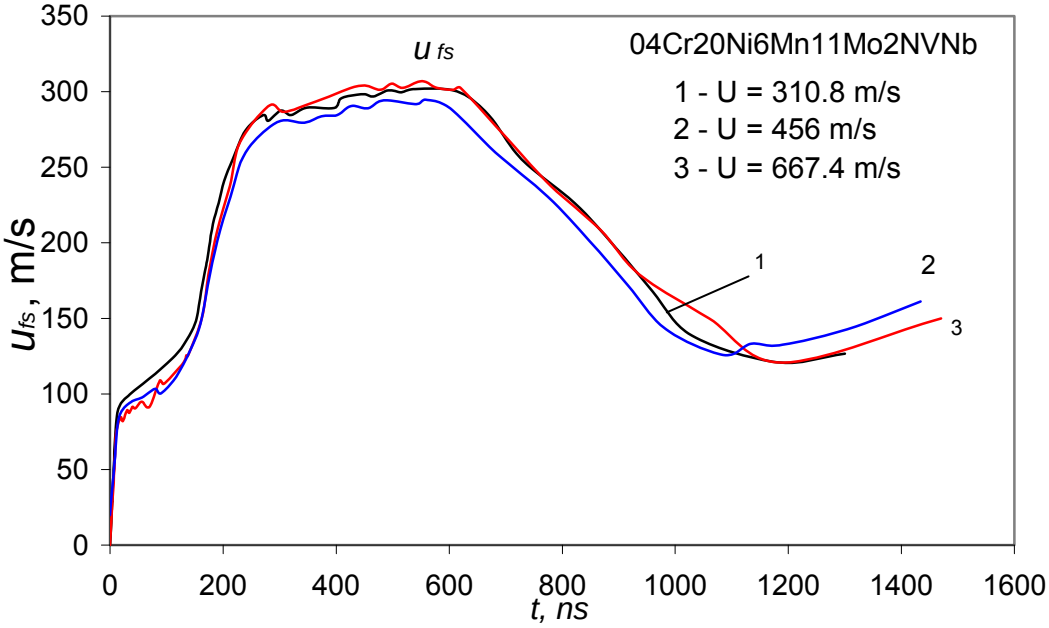

b)

Figure 8. Free surface velocity profiles for 30CrNi4M0 armor steel (a) and 04Cr20Ni6Mn11Mo2NVNb nitrogen steel (b).

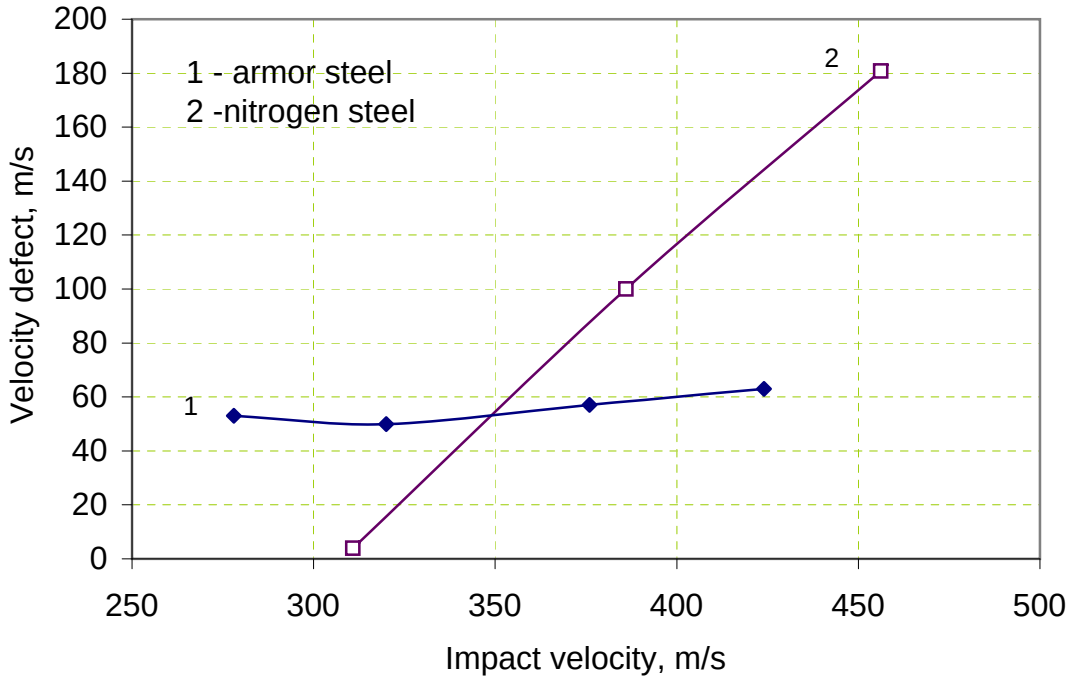

Figure 9. Defect of velocity versus impact velocity

which results in increase of threshold stress for structure-unstable state. It should be noted that just the structure instability threshold determines a resistance of material to high-velocity penetration (Meshcheryakov, 2004).

In ***Fig.10*** the cross-section micrographs of post shocked targets for both kinds of steel loaded at identical impact velocities of ~350 m/s are provided. Presence the mesoscale rotational cells (Fig.10 *a*) and particle velocity dispersion (Fig.8*a*) testifies a participating of mesoscale in dynamic deformation of Cr-Ni-Mo steel. On other hand, absence of velocity dispersion (Fig.8*b*) and uniform twinning mechanism of dynamic deformation in case of nitrogen steel (Fig.10*b*) evidences a direct transferring of external load from macroscale to microscale without participating the mesoscale.

At the same time, spall-strength for nitrogen steel proves by 20% higher than for Cr-Ni-Mo steel: 3.37 GPa and 4.16 GPa, respectively.

Thus, because of intermediate mechanisms of macro-meso energy exchange armor Cr-Ni-Mo steel has higher resistance to high-velocity penetration, whereas nitrogen steel has higher resistance to spallation.

In case of copper, post-shocked microstructure is quite different for the specimens loaded by scheme Fig.2*a* and Fig. 2*b*. When loaded on the first scheme, the specimen suffers a bending, which results in 3D deformation. In the second case, when specimen is pressed into copper ring, deformation is one-dimensional. 3D character of dynamic straining is known to facilitate the conditions for nucleation of stacking faults and twins *(Murr and Esquvel, 2004)*. Growth of plastic deformation at the expense of unlimited splitting of dislocations (motion of partial dislocations) with formation of twin lenses has been found by *Coujou (1983)* and theoretically analyzed by *Zaretsky (1995)*. It is shown that structures formed by system of splitting partial dislocations are the volumetrical 3D-formations of hpc-structure. Example of volumetrical piles in M3 copper is presented in ***Fig. 11***. In specimens tested by scheme Fig.2*a* the volumetrical formations of second phase are found to be uniformly distributed over the body of specimen, their dimensions increase with increase of impact velocity (see ***Fig.12***). Mean grain size for M3 copper equals 200÷300 μm, so each grain contains approximately 500÷1000 similar formations.

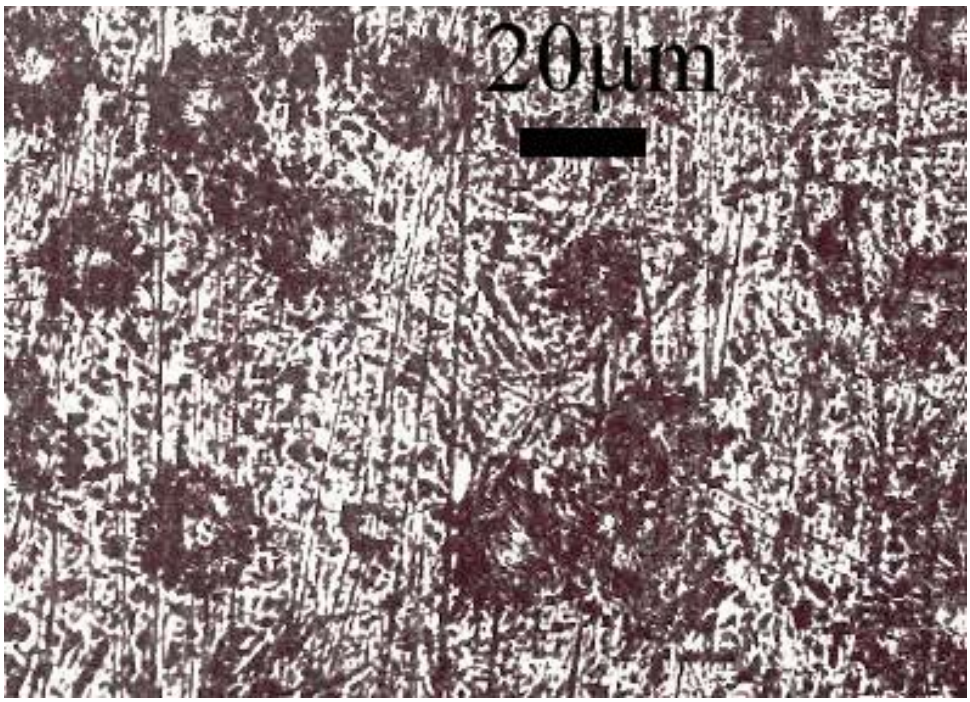

a)

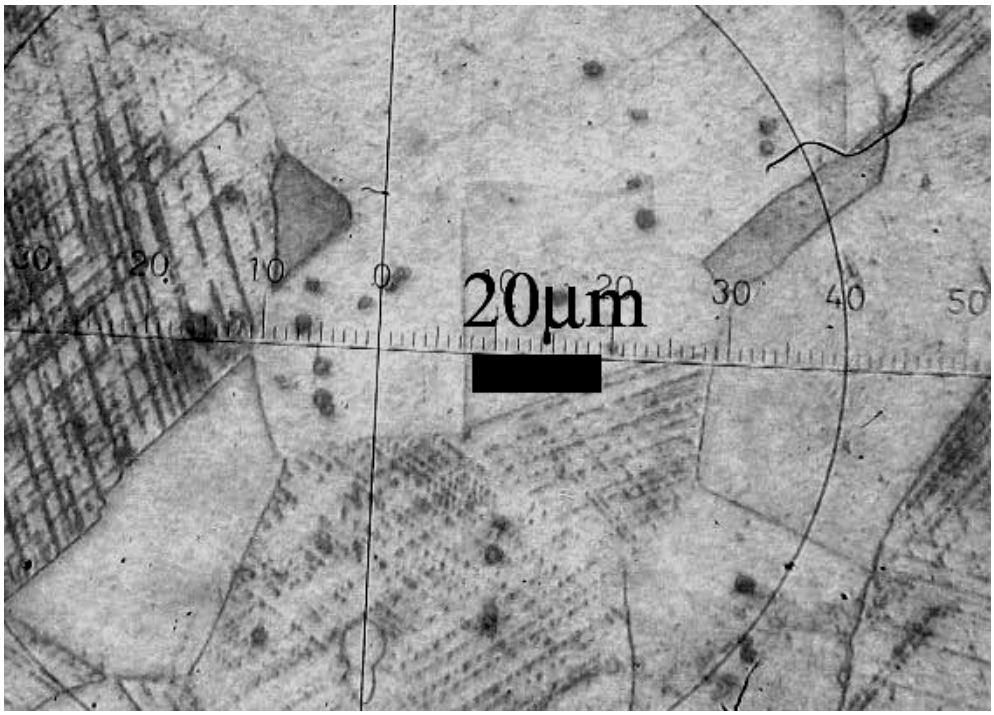

b)

Figure 10. Mesorotations in 30CrNi4Mo armor steel (a) and 04Cr20Ni6Mn11Mo2NVNb nitrogen steel (b) (impact velocity ~ 350 m/s)

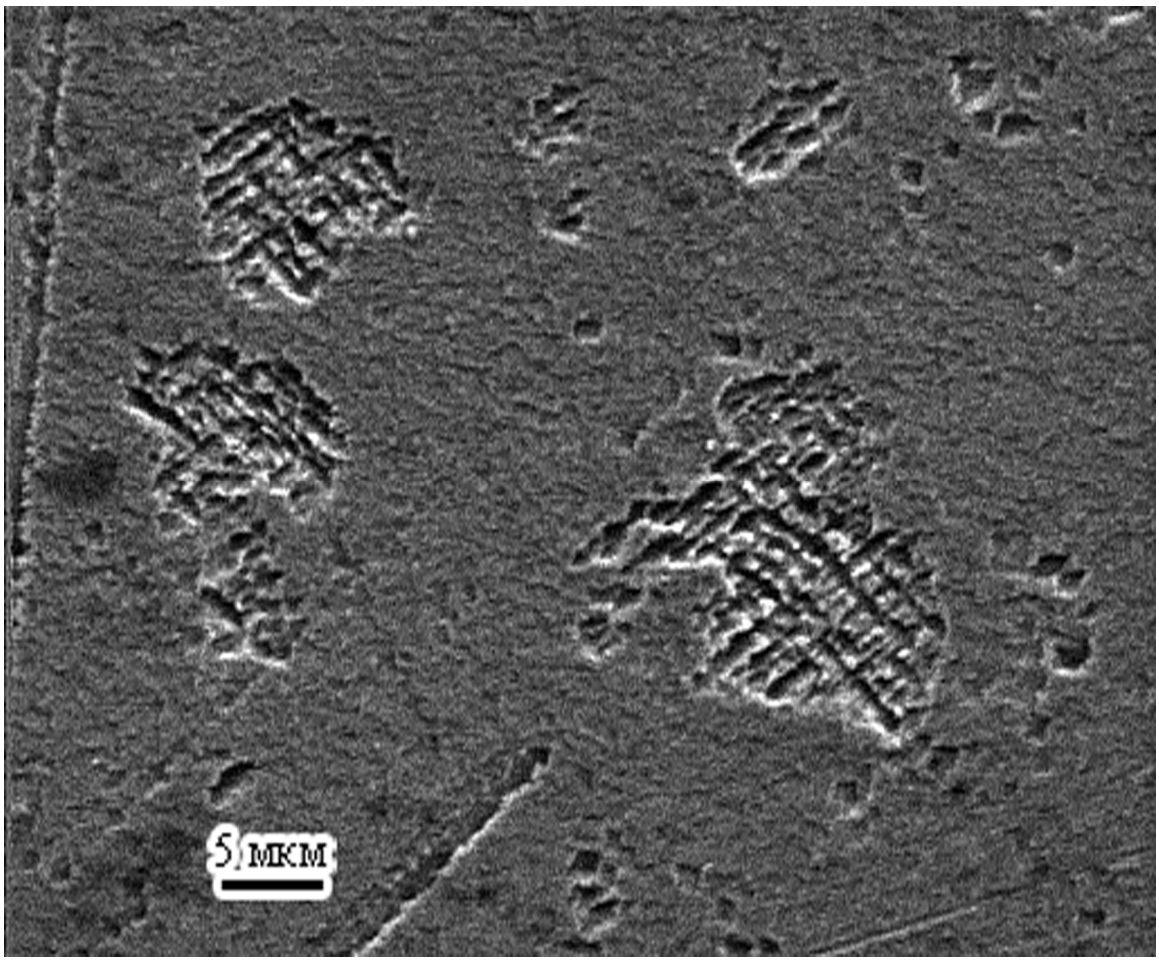

Figure 11. Twin lenses in M3 copper target

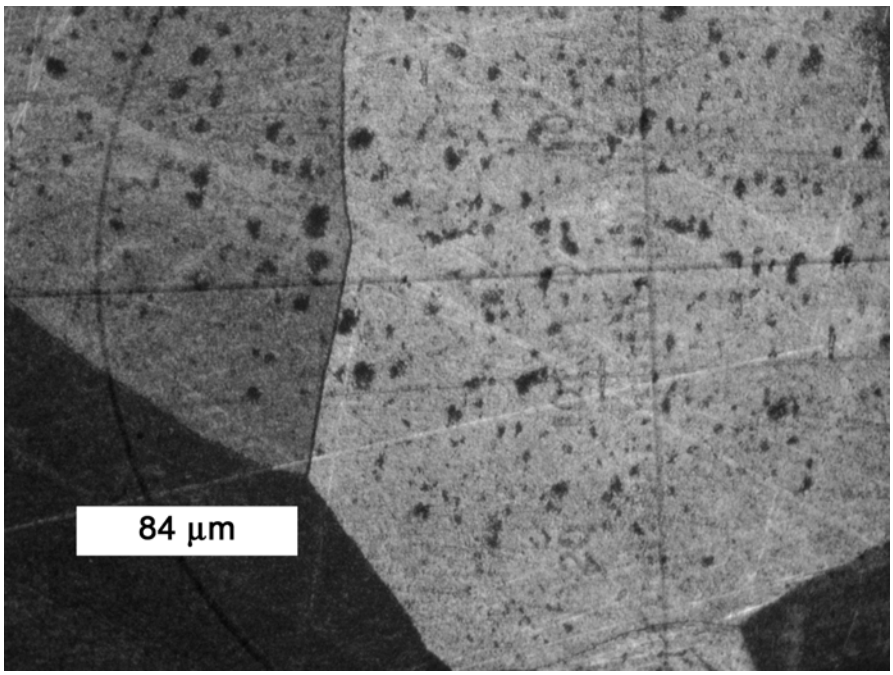

a)

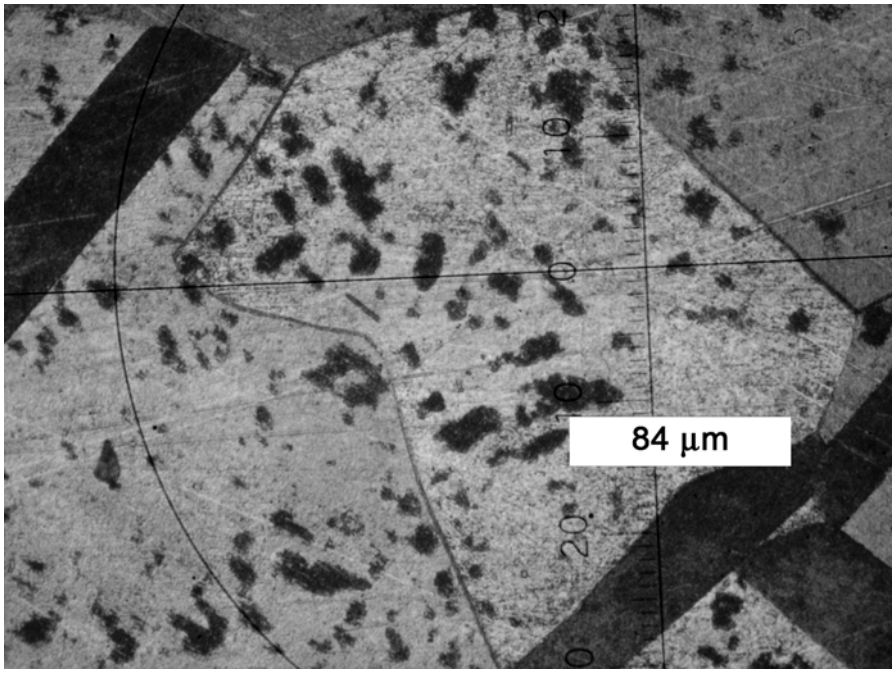

b)

Figure 12. Change of size of twin lenses depending on distance from loaded surface. a) 400 µm; b) 1400 µm.

Dependencies of formation mean size on distance from loaded surface for impact velocities of 400 m/s, 490 m/s and 500 m/s are presented in ***Fig.13***. It is seen that size of formations grows with distance, which means that rise-time of plastic front plays an important role in nucleation and growth of the formations. When plastic front becomes steady, so the rise-time of plastic wave is invariable, growth of formation delays as well. The twin formations shown in Figs. 9 correspond to equilibrium character of meso-macro exchange proper for *"Kolmogorov's universal equilibrium regime"*. Structures are sufficiently seldom distributed over the body, so they interact only with the medium while the mutual interaction between twin-structures is absent.

In 1D situation, which is proper for the second set of targets, the twinning is absent though the defect of particle velocity riches the same value. This means that meso-macro energy exchange continues to work even if visualization of vortical structures is not realized.

In the case of loading with explosive lens, the structure formation process turn out to be quite different. In ***Fig. 14*** a cross-section of copper target with turbulent-like formations is provided. The structures occupy the whole volume of grains favorable oriented respectively direction of loading. Interior of formation was shown to be the networks of microtwins *(Meshcheryakov, 2008)*, a micro-shear band morphology results from crystalline nature of deformation (see ***Figs. 15-16***).

Nucleation of dissipative structures occurs under simultaneous action of high pressure provided by uniaxial straining and shear along the crystalline planes. Physical mechanism for nucleation of dissipative structures is thought to be a resonance interaction between polarized periodical dislocation structure and space period of driving elastic-plastic wave. Since the parameters of shock waves were not measured in these experiments we cannot confirm above considerations, so further investigations are needed.

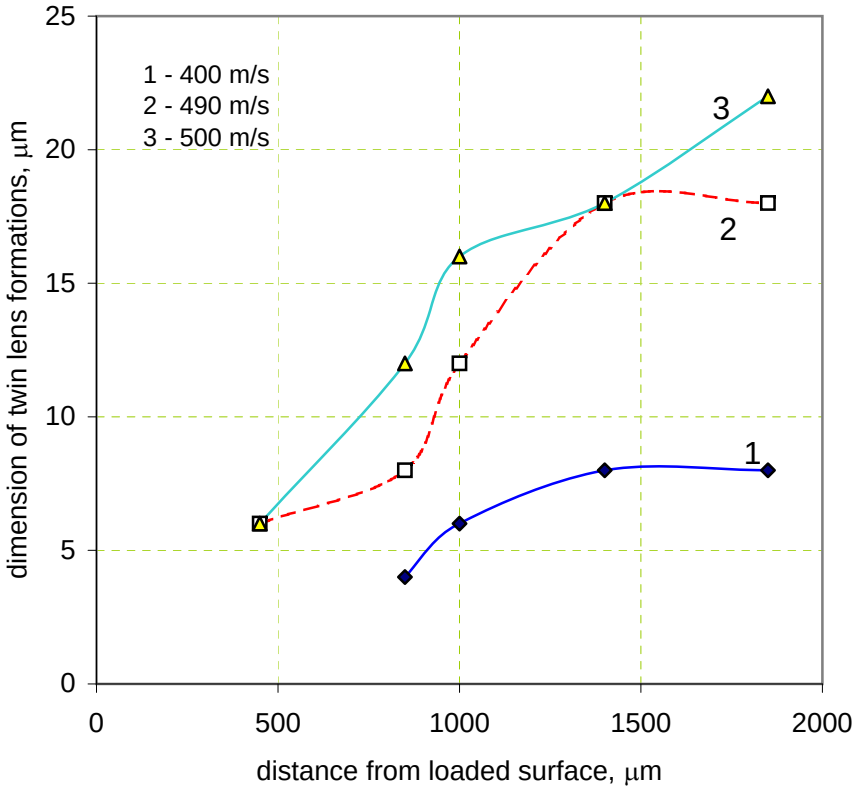

Figure 13. Dependencies of mean size of formation on distance from loaded surface for impact velocities of 400 m/s, 490 m/s and 500 m/s

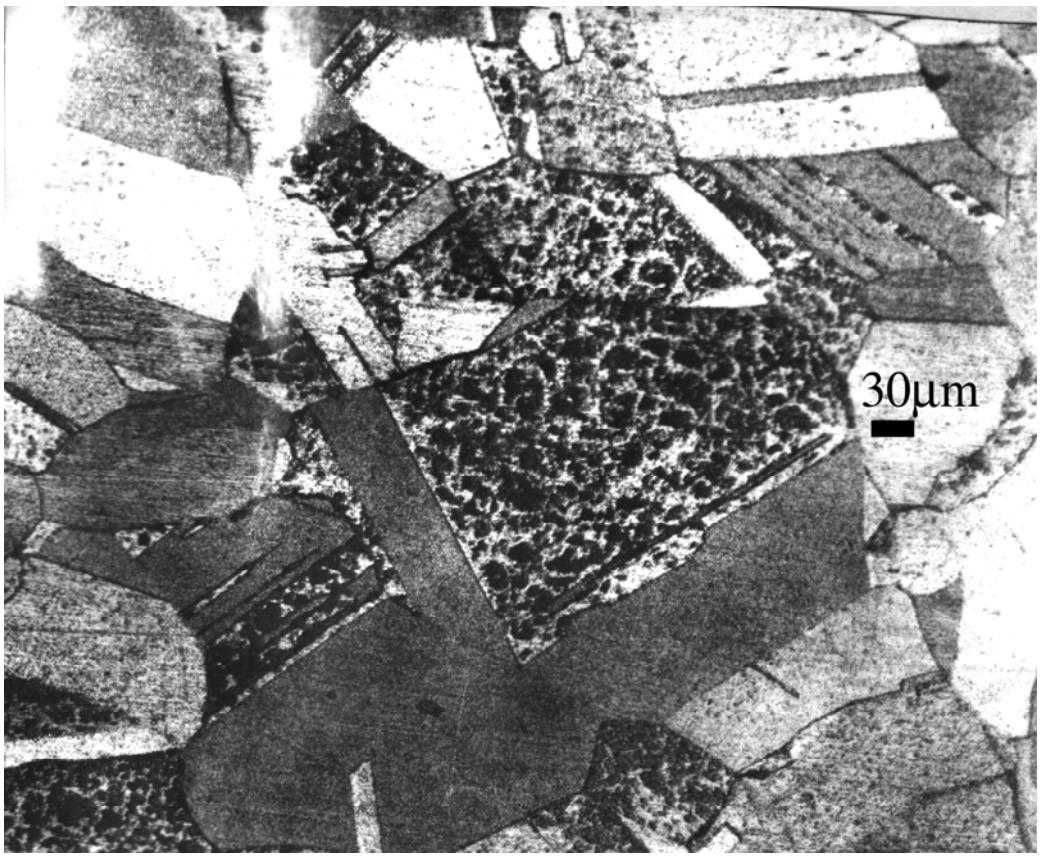

Figure 14. Cross-section of copper target with turbulent-like formations

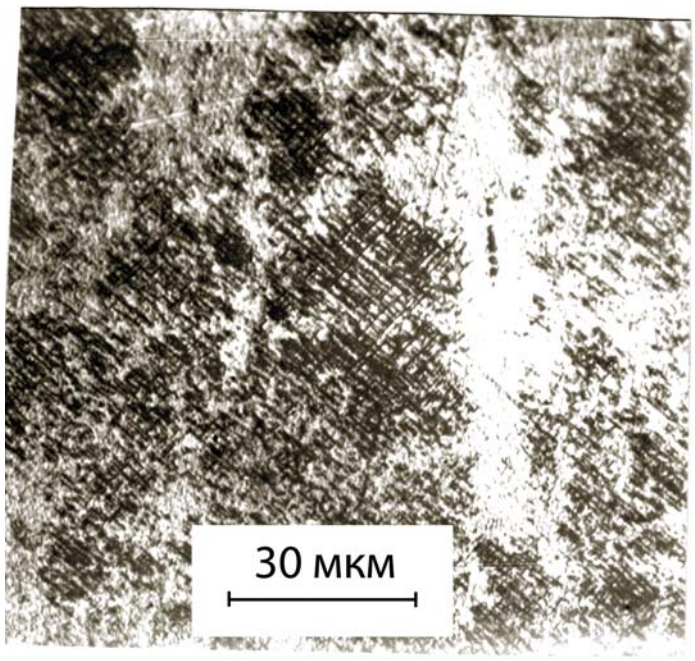

a)

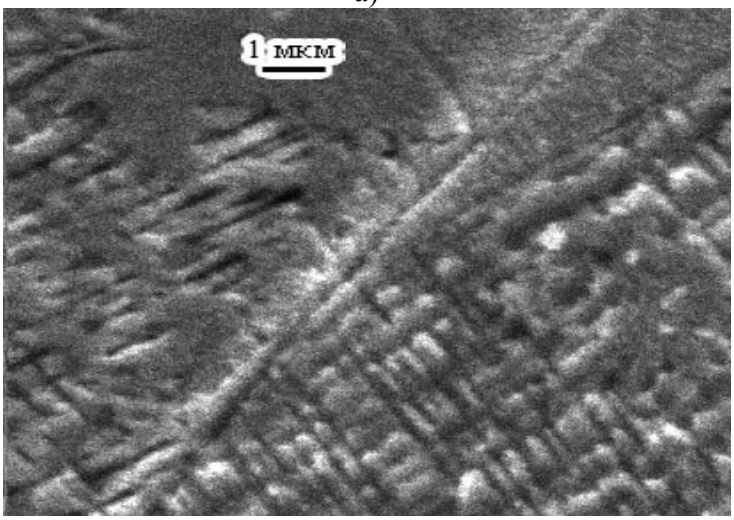

b)

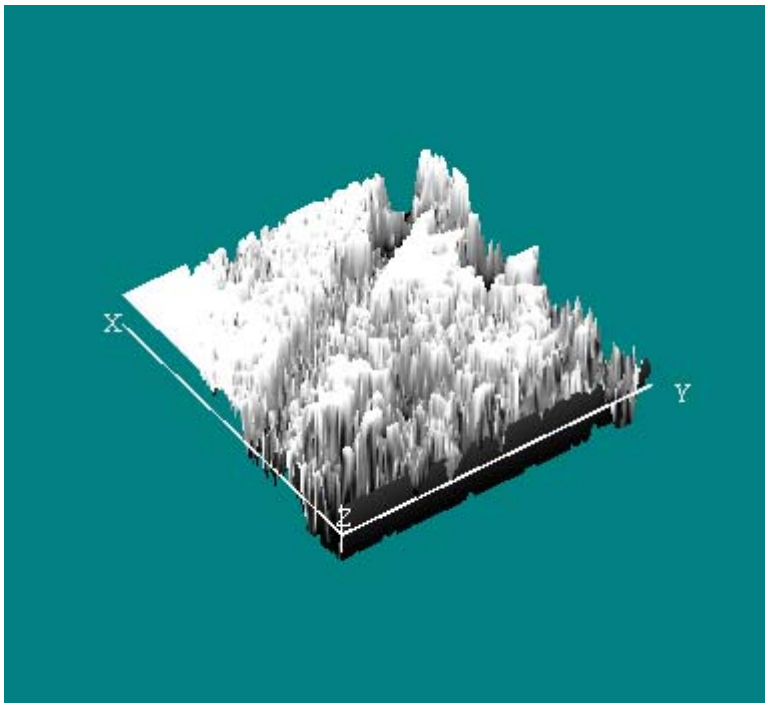

c)

Figure 15. Network of twin structures in M3 copper

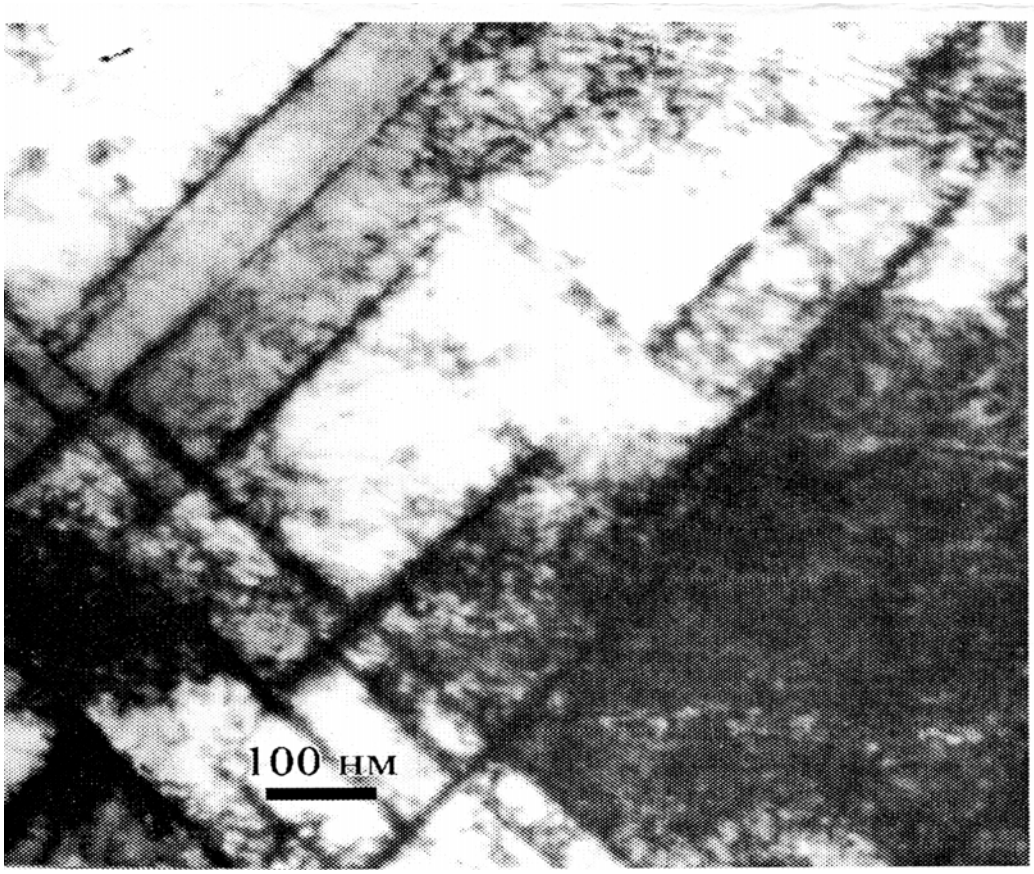

Figure 16. TEM – micrograph of twin network structure.

DISCUSSION

Specifics of shock-wave behavior of metals is a momentary transition into structure-unstable state *(Kanel et al.,1978; Skokov et al., 2008)*. According to Skokov et. al. (2008), duration of that state in copper is approximately 0.3÷0.5 μs. In the case of uniaxial straining, medium suffers high hydrodynamic pressure and shear. Analogous conditions are known to be realized in Bridgmen's chamber. The first stress component, high hydrodynamic pressure, transfers material to convective state, whereas the shear component realizes a motion of medium.

It should be underline that main measurable feature of transition of solid into structure-unstable state is a velocity defect. Volumetrical 3D structures in form of network twin formations is only ***a visualization*** of rotational motion of medium. The twin formations shown in Fig. 9 are not visualized, if stress state of medium doesn't provide the reciprocal component of shear stress during the shock wave passage. Just that situation takes place if the specimens are loaded in scheme Fig. 2*b*. In this case, after shock loading the grain structure remains invariable although velocity defect achieves the same value as for specimens loaded on scheme Fig.2*a*.

M3 copper transits into structure-unstable state at the impact velocity of ~310 m/s (point *A* in Fig.4). This impact velocity corresponds to strain rate where condition (9) is fulfilled. At the same time, into equilibrium regime of macro-meso energy exchange the material transits on at the impact velocity of 350 m/s when condition (3) is satisfied. In other words, for the optimum regime to be realized, it appears to be insufficient that material transits into structure-unstable state. It is necessary that the dynamic deformation enters into equilibrium regime of macro-meso energy exchange. For comparison, in ***Fig.17*** three stages of rotation cell forming in copper are presented. It is seen that central region of rotation cell is fractured and material is fragmented. In this case, the external energy expends not only on plastic straining but also on fracture of material. This situation is thought to be far from equilibrium regime of macro-meso energy exchange.

Figure 17. Successive stages of nucleation of rotational cell in copper.

CONCLUSIONS

As a result it can be concluded**:**

1. Shock tests of copper and steel under uniaxial strain conditions show that under certain relationship between rate of change of the velocity dispersion and macroscopic particle velocity material temporally transits in to structure-unstable state.
2. When strain rate at the mesoscale becomes equals the strain rate at the macroscale, plastic deformation enters into equilibrium regime of meso-macro energy exchange
3. In copper large-scale mesoscopic structures are visualized in form of nucleation of stacking fault lenses or microtwin network formations depending scheme of loading.
4. When material transits in to equilibrium regime of meso-macro energy exchange, dynamic strength achieves maximum possible value.
5. Depending on mechanism of energy exchange, material may reveal different dynamic strength. Participating of mesoscale in energy transferring increases resistance of material to high-velocity penetration. On the other hand, direct transferring of kinetic energy from macroscale to microscale increases resistance of material to spallation.

This work is conducting under support of RFBR grants: 08-02-00329 and 08-02-00304.

REFERENCES

Asay J.R., 2002. Shock Wave Paradigms and New Challengers. In: *"Shock Compression of Condensed Matter-2001"* Eds: M.D. Furnish, N.N. Thadhani, Y.Y. Horie. AIP Conference Proceedings 620. Melville, New York, pp.26-35.

Coujou A. 1983. Acta Metallurgica. **31**, No 10, 1505.

Hintze T. 1962. *Turbulence.* Mc Grow, New York. 546 p.

Kanel G.I., Dremin A.N., Molodets A.M., 1978. Change of strength of metals in shock wave. *Fizika metallov i metallovedenie.* **46,** 200-203 (Russian ed).

Mescheryakov Y.I., 1999. Mesoscopical effects and particle velocity distribution in shock compressed solids. In: *"Shock Compression of Condensed Matter-1999"* Eds: M.D. Furnish, L.C. Chhabildas, R.S. Nixon. AIP Conference Proceedings-505. Melville, New York. pp. 1065-1070.

Mescheryakov Yu.I. and. Divakov A.K., 1994. Kinetics of microstructure and strain-rate dependence of materials. *Dymat Journal*. **1**, No 4, 271-287.

Meshcheryakov Yu.I., Divakov A.K., Zhigacheva N.I, Makarevich I.P., Barakhtin B.K., 2008. Dynamic structures in shock-loaded copper. *Phys.Rev. B.* **78**, 64301-64316.

Meshcheryakov Yu.I., Divakov A.K., Zhigacheva N.I. 2004. Shock-induced structural transition and dynamic strength of solids. *Int. J. Solid and Structures.* **41**, 2349-2362.

Morosov N.F., Petrov Yu.V., Utkin A.A., 1991. On the structure-temporal approach in analysis of dynamic fracture of brittle mining rocks. *Proc. of Leningrad Mining Institute.* 125, 76-86 (Russian edition).

Murr L.E., and Esquvel E.V., 2004. Observations of common microstructural issues associated with dynamic deformation phenomena: Twins, microbands, grain size effects, shear bands and dynamic recrystallization. *J. Mat. Sci.* **39**, 1153-1168.

Skokov V.I., Ignatova O.N., Malyshev A.N., Podurets A.M., Raevsky V.A. and Zocher M.A., 2008. Temporal softening and its effect upon strength. In: *"Shock Compression of Condensed Matter-2007".* Eds: M. Elert, M.D. Furnish, R. Chau, N.C. Holmes, and J. Nguyen. AIP Conference Proceedings -955, 597-600.

Zaretsky E., 1995. Dislocation multiplication behind the shock front. *J. Appl. Phys*. **78**(6), 3740-3747.

"…Why the mesomechanics still doesn't incorporated in to shock wave process?"
(James R. Asay, 2002)

On-line experiments on multiscale dynamic plasticity are practically absent